J Appl Electrochem (2009) 39:2297–2313
DOI 10.1007/s10800-009-9939-6

Electrochemical microstructured reactors: design and application in organic synthesis

A. Ziogas · G. Kolb · M. O'Connell · A. Attour · F. Lapicque · M. Matlosz · S. Rode

Received: 15 August 2008 / Accepted: 3 June 2009 / Published online: 23 June 2009

Abstract The use of micro structured reactors is an accepted technology in fundamental chemical research as well as in industrial applications. The application of electrochemical microreactors (ECMR) has not attracted as much attention as continuously performed reactions in a confined space. Nevertheless ECMRs are in use to perform electro-organic reactions. In this review, different aspects of ECMRs with structured electrodes and interelectrode distances of mainly $\leq$100 μm are investigated and discussed, together with various manufacturing techniques and prototypes described therein. Based on representative examples described in various publications for electrolysis (for direct and indirect electrolysis) advantages and disadvantages of electrochemical microreactors are presented and compared with those of conventional electrochemical reactors.

Keywords Electrochemical microreactor · Paired electrosynthesis · Mass transfer · Current density distribution · Anodic oxidation · iR-drop

List of symbols

A_e	Electrode surface $A_e = Lw$ (m^2)
a_e	Volume specific electrode area (m^{-1})
a_{inv}	Specific investment costs (€/m^2 h)
A, B, C, D	Reagent or product of the electrochemical reaction
b_A	Kinetic constant of the reaction involving reagent A (V^{-1})
b_{inv}	Current costs (€/kW h)
C_A	Concentration of reagent A (mol m^{-3} or mol L^{-1})
D	Inter-electrode gap (m)
d_e	Electrode thickness (m)
d_{eq}	Equivalent or hydraulic diameter
D	Diffusion coefficient (m^2 s^{-1})
E^c, E^a	Cathodic, anodic potential (V)
E_e^c, E_e^a	Cathodic, anodic equilibrium potential (V)
E_{cell}	Cell voltage (V)
E_{tn}	Thermoneutral cell voltage
F	Faraday constant (96,486 A s mol^{-1})
i	Current density (A m^{-2})
I	Cell current (A)
I^*	Dimensionless cell current defined by Eq. 4 (–)
k_m	Mass transfer velocity (m s^{-1})
L	Electrode length (m)
M_P	Molar mass of product P (kg mol^{-1})
Z	Number of electrons involved (equiv mol^{-1})
$\dot{n}$	Molar flux (mol s^{-1})
NTU	Number of transfer units defined by Eq. 3 (–)
Q_{JOULE}	Heat generation flux (W)
Δp	Pressure drop bar
R_{cell}	Equivalent electrical cell resistance (Ω)
$R_{circuit}$	Equivalent resistance of the electrical circuit (Ω)
S_v	Distance relationship (–)
Sh	Sherwood number (–)
v_f	Superficial velocity of the liquid phase, $v_f = V_f/(dw)$ (m s^{-1})

A. Ziogas (✉) · G. Kolb · M. O'Connell
Institut fuer Mikrotechnik Mainz GmbH (IMM),
Carl-Zeiss-Str. 18-20, 55129 Mainz, Germany
e-mail: Ziogas@imm-mainz.de

A. Attour · F. Lapicque · M. Matlosz · S. Rode
Laboratoire des Sciences du Génie Chimique, CNRS-ENSIC,
BP 20451, 54001 Nancy, France

ΔU_{ohm}	Ohmic potential drop of the cell (V)
V_f	Electrolyte volumetric flow rate ($m^3\ s^{-1}$)
V_R	Reactor volume
w	Electrode width (m)
Wa	Wagner number defined by Eq. 5 (–)
X	Spatial coordinate (m)

Greek symbols

B	Current efficiency (–)
Γ	Aspect ratio of the channel (–)
η^a, η^c	Anodic, cathodic overpotential (V)
η_D	Dynamic viscosity (Pas)
k	Specific conductivity ($S\ m^{-1}$)
θ	Reagent conversion (–)
ρ_{ST}	Space–time yield ($kg\ m^{-3}\ s^{-1}$)
σ	Selectivity versus the desired product (–)
τ	Residence time (s)
Ψ	Product yield (–)
Ω	Specific electric energy consumption

Suffix

—	Space averaged value
in	Relative to the reactor inlet
out	Relative to the reactor outlet

Indices

∞	Relative to the bulk
i	Relative to the liquid–solid interface
lim	Limiting value
opt	Optimum value

1 Introduction

Electrolysis represents a tool for a number of material processing techniques and syntheses. While the main application of electrolysis takes place in the area of analytical [1, 2] and inorganic chemistry, there are instances of industrial electroorganic synthesis applications both in pilot plant and commercial scale status [3–7], performed mainly in conventional electrolyzers, with electrode distances of more than 1 cm.

Microreactors, in the broadest sense, involve process engineering components such as mixers, extractors, chemical reactors, evaporators, etc., which possess characteristic dimensions in the micrometer range.

Electrochemical microsystems and microreactors are best described according to their lateral and vertical dimensions as shown in Fig. 1 [6]. This can take the form

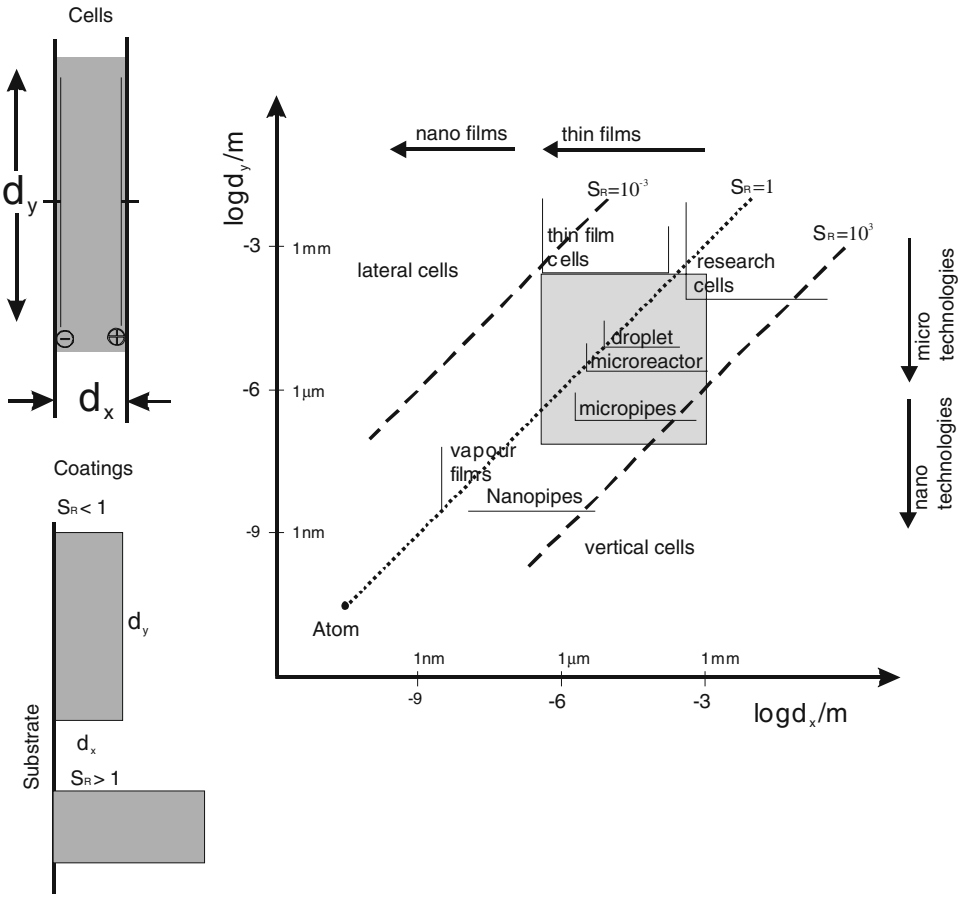

Fig. 1 Classification of electrochemical micro system technology with respect to the distance relationship S_V. *Dashed lines* show S_V of 10^{-3}, 1 and 10^3 respectively [6]

of a coating on the electrode surface or be concerned with the dimensions of an ECMR. The lateral direction (d_y) runs parallel to the electrode surface (y-direction) and the vertical direction (d_x) refers to the distance from the electrode surface or the distance between the electrodes.

The distance relationship S_V is defined as follows:

$$S_V = \frac{d_x}{d_y}. \quad (1)$$

Based on these characteristics and on the generally improved performance of microreactors [7], different ECMRs have been manufactured and evaluated in the last decade for electroorganic synthesis [8–16].

1.1 Reactors with microelectrodes for analytical and preparative use

Fleischman and co-workers [17] demonstrated that microelectrodes of radius <1 μm enable important electrochemical measurements to be made on uncharged organic, inorganic and organometallic compounds in a range of organic solvents (a) without addition of electrolyte, or (b) in the presence of very low concentrations of electrolyte either added deliberately or inadvertently present as impurities. Limitations apply to studies on charged species where migration currents are present. Fortunately, the great majority of compounds studied in organic solvents are uncharged species. Unfortunately, in their present format, microelectrodes are unsuitable for controlled-potential electrolysis experiments or other forms of bulk electrolysis as required in synthetic electrochemistry. These techniques would require an extensive array of microelectrodes, all of extremely small radii. Also new methods of electrode fabrication are required to solve such problems. The groups of Speiser and Schuhmann have successfully developed a computer-controlled instrument, based on scanning electrochemical microscope technology, that was employed in the miniaturized combinatorial electrosynthesis of localized compound collections [18, 19]. Libraries of iminoquinol ethers and triazolo-pyridinium ions were generated in the wells of microtiter plates by potentiostatic electrolysis. Several experimental protocols were described and implemented. Progress of the electrolyses was monitored by microelectrode steady-state voltammetry and product formation was screened by GC-MS or HPLC-MS.

1.2 Electrochemical flow reactors

Overviews of the various types of electrochemical cells that are of importance for industrial electrosynthesis processes as well as production schemes for organic electrosyntheses are given in different textbooks [20–25].

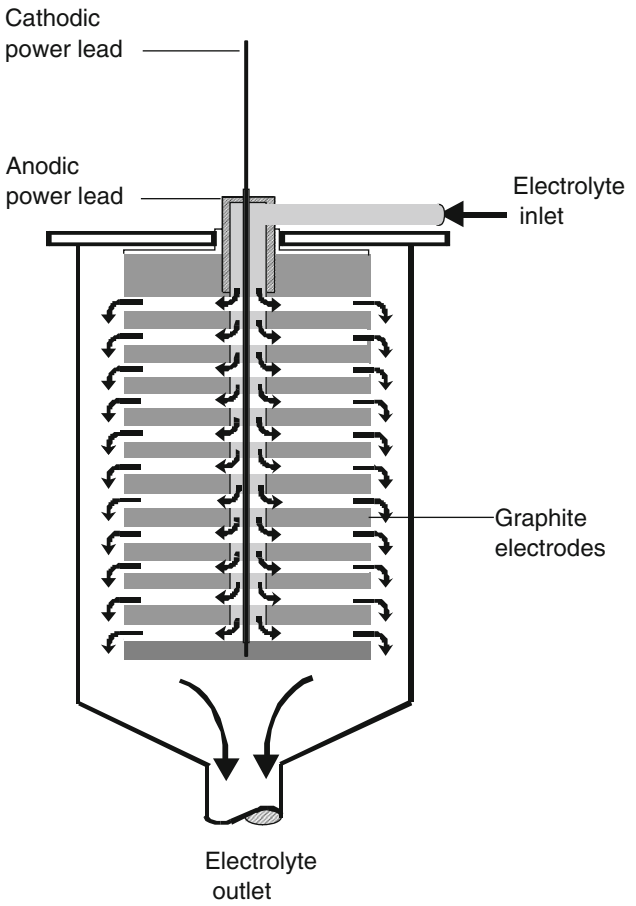

Fig. 2 Schematic view of an undivided electrochemical capillary gap cell [5]

A pioneering work for a later development of *E*lectro *C*hemical *M*icroflow *R*eactors ECMR was performed by Beck and Guthke [26] at the end of the sixties with the construction of the disc-stack capillary cell for anisaldehyde production with a gap of 0.2–1 mm [21, 26–28]. This type of cell as shown in Fig. 2 is used commercially for many varied electroorganic applications with additional possibilities of "paired electrolysis" with simultaneous formation of valuable products at the anode and cathode [20]. In the majority of these industrial cell types the interelectrode gap is in the millimetre range (1–2 mm).

Previous reports [8, 10] have described the high performance and the related benefits of electrochemical microreactors. High performance in this context means that higher conversion, product yield and selectivity in shorter residence times, i.e. higher space–time yields, can be achieved in ECMRs compared to classical electrochemical reactors. Furthermore higher current efficiency can be obtained.

This high performance originates from the operational advantages, which can be expressed in terms of even uniform mass transport distribution, fast heat exchange and effective temperature control, uniform current density

distribution and effective current control. Finally, the reduction of conductivity salt and energy consumption combined with the possibility of a simple scaling up procedure, are important reasons to utilise ECMRs. In brief the combination of all these properties emphasizes the benefits of ECMRs compared to conventional ECR.

Due to technical conditions and the constitution of electrolytes and electrodes in the case of parallel electrodes and a uniform current density distribution, a current increase is associated with a corresponding ohmic resistance as described in Eq. 2.

$$\Delta U = IR_{drop} = I\frac{1}{A_e}\frac{d}{\kappa} = i\frac{d}{\kappa} \tag{2}$$

where ΔU is the potential drop between the electrodes, I the current, R_{drop} the electrolyte ohmic resistance, A_e the electrode surface, d the distance between the electrodes, κ the specific ionic conductivity and i the current density respectively.

It is obvious from Eq. 2 that if the electrode gap is reduced by a factor of 400 the conductivity of the electrolytes can be similarly lowered by a factor of 400 on equivalently even current distribution. This is easily achieved via reduction of the conducting salt concentration.

For the operation of electrolysis plants, it is of great significance that the depletion of the electroactive component concentration in the bulk solution is as small as possible, the diffusion layer remains as thin as possible and the concentration of the component tends to zero at the electrode surface. The material disadvantages of the most conventional electrochemical reactors compared to ECMRs consist of large dimensioned housing and thick electrodes and gaskets which can result in small volume to surface ratios and lower space–time yields.

1.3 Use of ionic liquids in ECMR

Normally water cannot be used as the solvent owing to the low solubility of the electroactive organic substances, its relatively small potential window i.e. its low anodic and cathodic decomposition potential and its amphoteric character, which frequently gives cause for solvolysis and decomposition reactions of organic substances [21–23].

The use of ionic liquids in organic electrochemistry in the last decade has opened up new opportunities, not only in electroanalytical chemistry but also in the electroorganic synthesis using micro reactors [27]. Air and moisture stable ionic liquids such as 1-ethyl-3-methylimidazolium trifluoromethanesulfonate ($EMICF_3SO_3$) have been used as electrolyte for the electrooxidative polymerization of pyrrole [29]. The morphological structure of polypyrrole film formed on the anode was greatly affected, and the polymerization rate, electrochemical capacity and electroconductivity were significantly increased. Furthermore, it was also found that $EMICF_3SO_3$ could be recovered by a simple extraction of the remaining pyrrole monomer from the ionic liquid after use, and then reused without significant loss of reactivity for the polymerization. However, unlike the use of aqueous electrolytic solutions, the use of organic solvents is associated with a significantly reduced specific conductivity. Therefore it is especially important, for efficient electroorganic syntheses, that the cells are manufactured with a minimal gap between the electrodes.

1.4 Model reactions for the testing of ECMR

Several model reactions have been dealt with in the literature to emphasise the benefits of ECMRs versus conventional cells with and without supporting electrolyte [10, 14–16]. Two reactions, in particular, have been chosen for modelling of new microreactors as compared to model reactions for industrial production.

(1) The direct anodic oxidation of 4-methylanisol to 4-methoxy-benzaldehyde-dimethylacetal in methanol.

This reaction is important in industrial organic electrochemistry, due to the wide use of the resulting aldehyde as a precursor for fine chemical production, such as pharmaceuticals, dye-stuffs, plating additives, pesticides and flavour ingredients [20, 23–26, 28, 30–34].

(2) The direct and indirect anodic oxidation of furan to 2,5 dimethoxy-2,5-dihydrofurane in methanol.

2,5-Dimethoxy-2,5-dihydrofurane is an important disinfectant and can be produced by chemical or electrochemical methods. Because of poor space–time yields and considerable problems with work up and recycling of the electrolyte, indirect electrochemical processes generally have not been established industrially [34]. Nevertheless a strong reduction of the bromide mediator and the single-pass continuous mode operation of the ECMR eliminate many of the difficulties observed with conventional ECRs and realise new opportunities for ECMR's.

In this review which is based on representative examples described in diverse publications for electrolysis, the advantages and disadvantages of electrochemical microreactors are presented and compared with conventional electrochemical reactors.

2 Electrochemical flow microreactor

2.1 Principle of the micro-structured single-pass conversion reactor

An important aspect of the construction of electro-chemical micro reactors is the attainment of high current densities

over the whole electrode surface and the achievement of a homogeneous potential between the electrodes. Current distribution depends on the cell and electrode geometry and therefore the construction of flow-through micro reactors with flat, parallel and equal surface area usually leads to low conversion and to a uniform current distribution. Operations in single-pass high conversion reactor lead mostly to non-uniform current density distributions. The best operational conditions are achieved by uniform overpotential distributions.

A major interest of micro-plate and channel reactors is related to the high specific area which permits operation in a single-pass high conversion mode, leading to a continuous process without recycle. This process scheme has two major advantages over classical process flow schemes [20]: it requires only a small separation unit and both the short residence time and the plug flow of the reagent minimize undesired side reactions [35].

2.2 Manufacture of electrochemical micro reactors

Parallel to the use of thin layer technology and the adoption of micro structuring procedures, microreactors for electrochemical synthesis have been developed and evaluated.

2.2.1 One channel thin gap cells

Many of the microreactors used for electroorganic synthesis are very simple.

Thin layer flow cells are constructed from different plates of materials such as platinum, lead dioxide, glassy carbon, graphite, nickel, indium-tin oxide, etc. as anode and platinum, silver, lead, stainless steel, glassy carbon, graphite etc. as cathode. A spacer (on both sides adhesive tape, 80–320 μm thickness) to leave a rectangular channel and the two electrodes are sandwiched together as shown in Fig. 3 [14]. After connecting Teflon or silicon tubes to the inlet and outlet the cell is sealed with epoxy resin. The flow rate of the reaction solution was controlled by using a plunger as a pump [11–14].

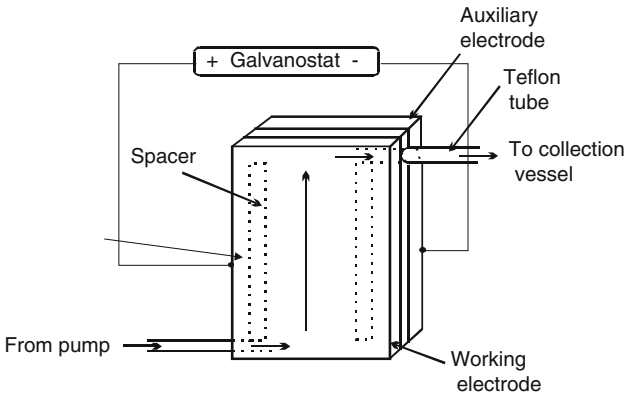

Fig. 3 Schematic illustration of the one channel micro-flow reactor [14]

In general, the scale up of electrochemical reactions and the production of electrodes, cells. spacers and separators requires several different technologies and materials. An overview of some technologies used in IMM is provided in Table 1.

Comninellis and co-workers reported the use of Boron doped diamond electrodes. Such electrodes are characterized by high resistivity and high hydrogen and oxygen overvoltage. The use of such electrodes in water makes available an exceptionally wide potential window [36–38].

Laser technology is a very good tool for easy, fast and cheap manufacture of electrodes. Cutting of graphite, glassy carbon or different metal electrodes, as well as structuring of the electrode surface, is possible with good accuracy. Laser techniques are suitable for planar structures, while the LIGA process (synchrotron radiation lithography, galvanoforming, and plastic moulding) is the best for the fabrication of microstructures with high aspect ratios and large structural heights [6, 7].

2.2.2 Multichannel ECMR of IMM

The ECMR consists of cathodes with an integrated heat exchanger and a 1 mm thick anode as well as Karlez®, a perfluored elastomer (DuPont, Germany), as seals. A 25 μm thick Capton® (polyimide) slit foil is pre-structured by laser treatment [10, 39]. The Capton® foil is then mounted between two flat electrodes and this assembly forms the channels of the micro cell (first version) To address the fixing problems of the chemically and electrically inert foil the cathodes are coated with PTFE-layers of well-defined thickness (100 μm second version). These layers were structured subsequently leading to immobilized spacers. Figure 4 provides one example of the set-up of ECMR. This construction allows for different operational modes. It is possible to run the reactor in series or parallel mode. Moreover, this kind of construction enables the building of a stack of mono and bipolar cells with or without integrated heat exchangers and shows excellent mechanical stability (stable up to a pressure of 65 bar and to a temperature of 200 °C).

For electrical insulation the stainless steel housing was also coated with PTFE. The picture of the coated reactor is shown in Fig. 5. This ECMR model was built with different electrode materials such as graphite, glassy carbon, platinum, nickel, lead and lead oxide. The process parameters and experimental results of the reactors were reported previously [10, 40] and are provided in Table 2 in comparison to the industrial process as in Table 3 [35].

Table 1 Different available materials and techniques used at IMM GmbH for the micro structuring and manufacturing of ECMR

Materials	PCM/PECM	LIGA	Casting/milling	Laser-cutting	μ-EDM-cutting	Etching
Carbon/graphite	+	−	+	+	+	+
Ceramics	+	+	+	+	+	+
Glassy carbon	+	−	−	+	+	−
Gold	+	+	+	+	+	+
Pb/PbO_2	+	+	+	+	+	+
Ni/NiO	+	+	+	+	+	+
Ebonex® (Ti_4O_7/Ti_5O_9) suboxides Magneli phase[a]	−	−	−	+	+	−
Platin	+	−	+	+	+	−
Boron doped diamond/graphite	+	−	+	+	+	−
Platinated titanium	+	−	−	+	+	−
Stainless steel	+	−	+	+	+	+
Cu	+	+	+	+	+	+
Cadmium	+	−	−	+	+	−
Hg	−	−	−	−	−	−
Capton®	+	−	−	+	−	−
Teflon® coating	+	−	+	+[b]	−	−
Nafion®	+	−	−	+	−	−
SPEEK	−	−	−	−	−	−
25% glassy fibre-PTFE	−	−	+	−	−	−
PEEK	−	−	+	−	−	−
PC	−	−	+	+	−	−
Viton®	−	−	−	+	−	−
Karlez®	−	−	−	+	−	−
Chemraz®	−	−	−	+	−	−

PCM/PECM Photochemical machining/electrochemically supported, *LIGA* lithography galvanic moulding, *μ-EDM* micro-electro discharge machining

[a] Magnéli phases are a range of substoichiometric oxides of titanium of the general formula Ti_nO_{2n-1} (where n is between 4 and 10) produced from high temperature reduction of titania in a hydrogen atmosphere. These blue/black ceramic materials exhibit conductivity comparable to that of graphite and can be produced in a number of forms, such as tiles, rods, fibres, foams and powders. While these materials have been studied for many years, they have only recently received interest for use as ceramic electrode materials, commercially termed 'Ebonex®', and are beginning to challenge precious metal coated anodes for some applications in aggressive electrolytes [34, 52–54]

[b] NdYAG laser ~70 W; $\lambda = 1{,}064$ nm

2.3 Mass transfer and overall performance process parameters

Rode et al. have developed a dimensionless reactor model for the electrosynthesis of anisaldehyde which describes the performance of an electrochemical single-pass, high-conversion reactor as a function of the reaction kinetics and of three independent, dimensionless parameters: the dimensionless current I^*, the Wagner number Wa, and the number of transfer units (NTU) [35, 39, 41, 42]. The reaction scheme for the anodic methoxylation of 4-methoxy toluene is shown in Fig. 6

$$NTU = \frac{k_m A_e}{V_f} \tag{3}$$

$$I^* = \frac{I}{(z_A + z_B) F V_f C_{A_0}} \tag{4}$$

$$Wa = \frac{\kappa_{eq}}{z_A F k_m C_{A_0} db_A} \,. \tag{5}$$

The dimensionless concentrations and the dimensionless spatial coordinate are defined as:

$$C_j^*(x^*) = \frac{C_j(x^*)}{C_{A_0}} \tag{6}$$

$$x^* = \frac{x}{L}. \tag{7}$$

Other dimensionless parameters defined in the model are the dimensionless current density of component j (j = A, B or C) (Eq. 9) and the total local current density (Eq. 10) for the desired oxidation reactions (Eq. 11)

$$i_j^*(x^*) = \frac{i_j(x^*)}{z_A F k_m C_{A_0}} \tag{8}$$

$$i_{Gl}^*(x^*) \quad = i_A^*(x^*) + i_B^*(x^*) + i_C^*(x^*). \tag{9}$$

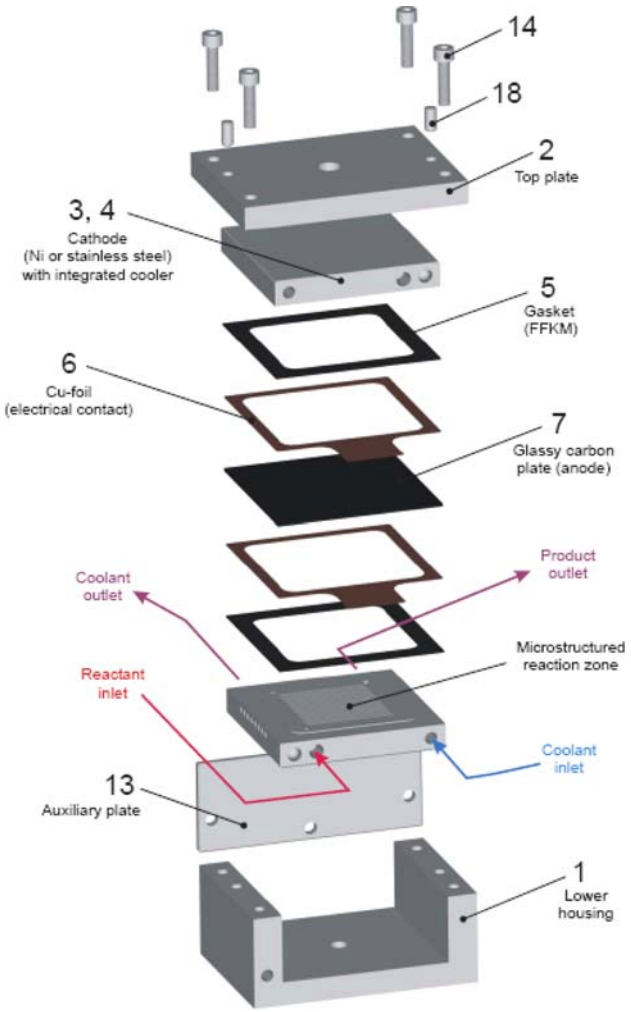

Fig. 4 Exploded view of ECMR showing the components which are comprised of an anode made from glassy carbon and cathodes made from stainless steel (*source*: IMM)

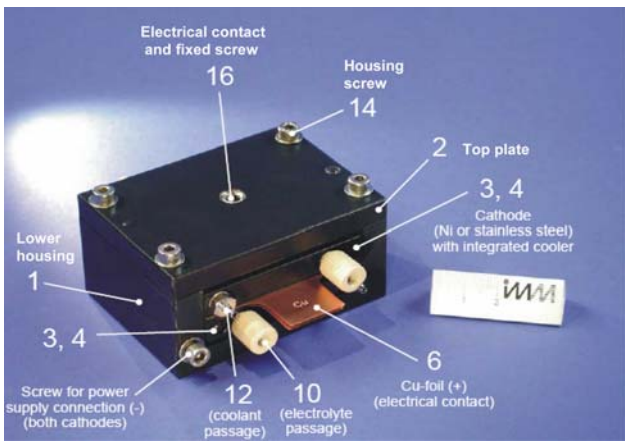

Fig. 5 Photo of the modified PTFE coated ECMR (ELMI®) (*source*: IMM)

A single-pass high-conversion electrochemical cell should operate ideally at a dimensionless current close to unity, permitting high yields at high current efficiencies. Dimensionless currents higher than unity are not desirable in principle as they are always associated with current efficiencies lower than unity. Furthermore, if the secondary reactions involve the desired product, dimensionless currents higher than unity lead to a rapid decrease in product yield.

High reagent conversions imply *NTU*s higher than unity. For the methoxylation of 4-methoxy-toluene to anisaldehyde, a reasonable *NTU* is 10–12. Lower *NTU*s do not permit complete conversion of the reactant, and lead to a reduction in the maximum attainable selectivity. Higher *NTU*s diminish the space–time yield without further increasing the reactor performance.

The Wagner-number is the relevant dimensionless quantity that determines current density distributions. Low Wagner numbers lead to uniform current density distributions over the electrode length, whereas high Wagner numbers induce uniform overpotential distributions.

Figure 7 illustrates the dimensionless current-density distributions in the electrochemical reactor for $I^* = 1$. The empty symbols correspond to the limiting behaviour of the system for high Wagner numbers ($1/Wa \rightarrow 0$) whereas the filled symbols correspond to the limiting behaviour at low Wagner numbers, i.e. $Wa = 0.002$. The circles represent calculations performed for $NTU = 6$, whereas the triangles represent calculations performed for $NTU = 12$.

A thin-gap microreactor was used to compare the simulation with the experimental results (see Sect. 2.2.2). The 100 μm thin-gap cell was operated with initial reagent concentrations of 0.1 and 0.01 M of potassium fluoride as supporting electrolyte at ambient temperature and pressure. Full conversion and selectivities exceeding 90% were obtained at a liquid flow rate of 0.1 mL min^{-1}, corresponding to an NTU of approximately 12. The above statements are only valid for the particular case of large conversions in the flow cell.

2.4 Space–time yield

For the global reaction performed in a continuous flow reactor in steady-state flow,

$$A \rightarrow B + ze^- \tag{10}$$

the reagent conversion θ, product selectivity σ and material yield Ψ are defined respectively by:

$$\theta = \frac{\dot{n}_A^{in} - \dot{n}_A^{out}}{\dot{n}_A^{in}} \tag{11}$$

$$\sigma = \frac{\dot{n}_B^{out}}{\dot{n}_A^{in} - \dot{n}_A^{out}} \tag{12}$$

Table 2 Brief overview of the ECMR-25 μm dimensions, the process parameters and results achieved for the electroorganic synthesis of anisaldehyde [10]

Microreactor dimensions	Value	Process parameters of ECMR[a]	
Channel length	$2 \times 3.2\ 10^{-2}$ m	Electrode material	Anode: GC
Channel width	8×10^{-4} m		Cathode: stainless-steel
Channel surface	5.12×10^{-5} m^2		
Channel height or electrode distance	25×10^{-6} m	Overall process flow scheme	Single-pass high-conversion
Channel volume	1.28×10^{-9} m^3	Electrolyte flow rate	1.67×10^{-9} m^3 s^{-1}
Number of channels	27		
Total active electrode surface	1.38×10^{-3} m^2	Residence time, τ	20.7 s
Total active reactor volume, V_R	34.6×10^{-9} m^3	Inlet concentration of the electroactive component	0.1–2 × 103 mol m^{-3}
a_e-value	40,000 m^{-1}	Supporting electrolyte concentration	10 mol m^{-3} (−)[b]
		Average mass transport coefficient, $\overline{k_m}$	1.07×10^{-4} m s^{-1}
		Operating pressure (maximum tested pressure)	1.1 bar (65 bar)
		Operating temperature	10–60 °C
		Reactor voltage	4–5 V (>7 V)[b]
		Current yield, β	>90% (67%)[b]
		Overall conversion, θ	90–98% (27%)[b]
		Selectivity, σ	>85% (> 95%)[b]
		Material yield (σ*θ)	>80%

Heat exchanger[b]	Value	Process parameters of the heat exchanger
Channel length	4.2×10^{-2} m	Cooling medium (water) flow rate system dependent
Channel diameter	$2.38\ 10^{-3}$ m	
Number of channels	8	

[a] First model with PC housing and without integrated heat exchanger

[b] In the absence of supporting electrolyte

Table 3 Comparsion between the BASF process as described in reference [20] and measurements performed with the high pressure cell [35]

Process parameters	BASF industrial process [20]	Experiments in the high-pressure-cell [35]
Overall process flow scheme	Continuous with recycle	Single-pass high-conversion
Electrode material	Bipolar graphite rings	Glassy carbon anode
		Stainless steal cathode
Inter-electrode gap	0.5×10^{-3}–1×10^{-3} m	0.1×10^{-3} m
4-methoxytoluene inlet concentration	10–25 mass% (0.65×10^{-3}–1.65×10^{-3} mol m^{-3})	7.5 mass% (0.5 × 103 mol m^{-3})
Supporting electrolyte concentration	0.3–3 mass%	0.07 mass%
	Potassium fluoride	Potassium fluoride
	Sodium sulfonate	0.01×10^{-3} mol m^{-3}
Operating pressure	Atmospheric	5 bar
Operating temperature	40–50 °C	45 °C
Current density	300–500 A m^{-2}	510 A m^{-2}
Voltage per gap	4–6 V	7 V
Current yield, β	Not indicated	85%
Overall conversion, θ	90–99%	90%
Selectivity, σ	85%	92%
Material yield ($\psi = \sigma * \theta$)	>80%	82%

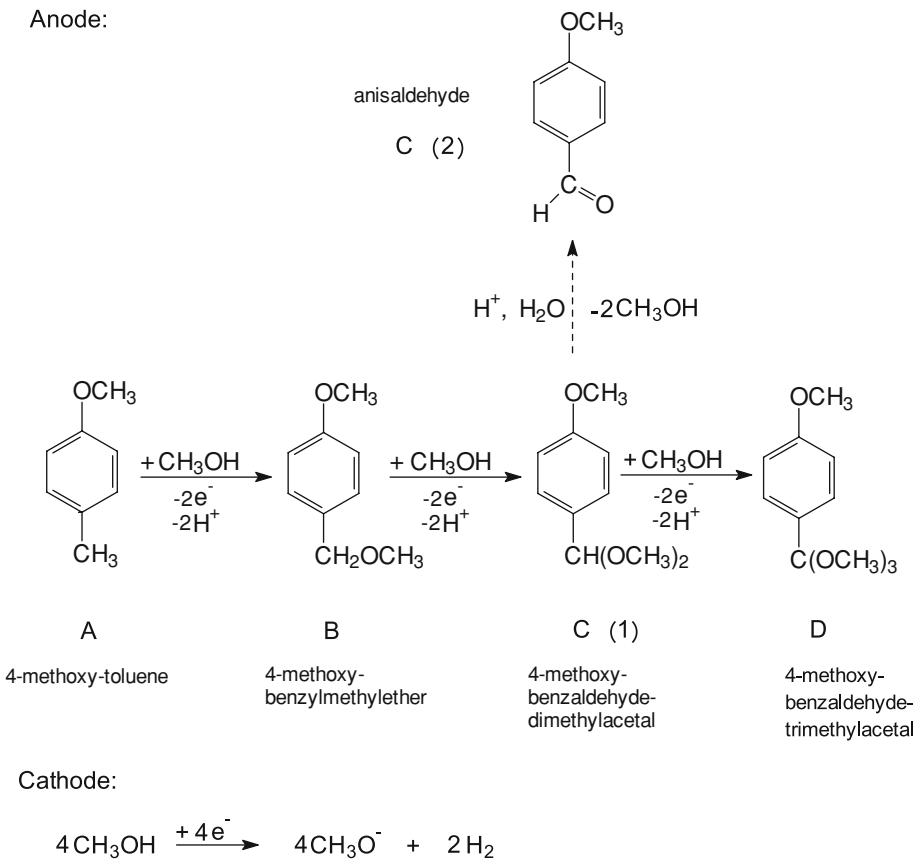

Fig. 6 Anodic oxidation of 4-methoxy-toluene to 4-methoxy-benzaldehyde-dimethylacetal

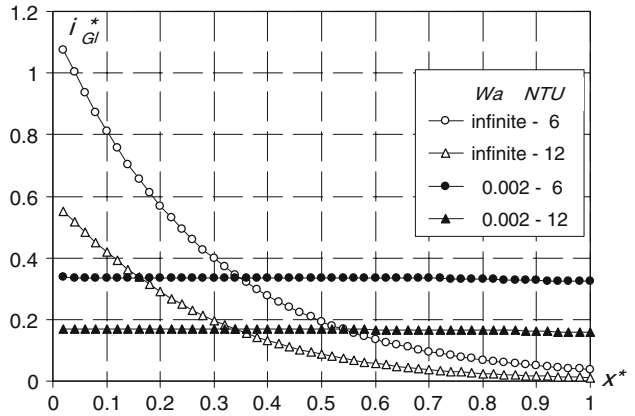

Fig. 7 Dimensionless current density ($i^*_{Gl}(x^*)$) distributions in the electrochemical cell for limiting Wagner numbers and for different NTU's; $I^* = 1$ [35]

$$\psi = \frac{\dot{n}_B^{out}}{\dot{n}_A^{in}}. \tag{13}$$

The dimensionless current can be defined as the ratio of the applied current to the current necessary to entirely convert the reagent flux:

$$I^* = \frac{I}{zF\dot{n}_A^{in}} = \frac{I}{zFC_A^{in}V_f} = \frac{\psi}{\beta}. \tag{14}$$

One of the most valuable indicators of reactor performance for steady-state conditions is the space–time yield, which expresses the mass amount of product per unit time and reactor volume V_R

$$\rho_{ST} = \frac{M_P\dot{n}_P^{out}}{V_R} = \frac{M_P\left(C_A^{in} - C_A^{out}\right)}{\tau} = \frac{M_P a_e i\beta}{zF} \tag{15}$$

where $\tau = V_R/V_f$, $a_e = A_e/V_R = d^{-1}$, M_P is the molar mass of the product and β is the current yield defined as:

$$\beta = \frac{zF\dot{n}_P^{out}}{I}. \tag{16}$$

For fully developed laminar flow between two electrode plates a limiting Sherwood number is $Sh_{lim} = 2.69$ [41, 42]. The space–time yield can be expressed in a single-pass high conversion cell ($I^* = 1$, $NTU = 10$) as [35, 41–43]:

$$\rho_{ST} = \frac{I^*\beta}{NTU}\frac{M_P k_m \overline{C}_A}{d} \cong 0.269\beta\frac{M_P D\overline{C}_A}{d^2}. \tag{17}$$

Equation 20 shows that reduction of the inter-electrode gap leads to enhancement of the attainable space–time yield. Moreover, it can be shown that, for a given electrolyte conductivity, process intensification is achieved without increasing the ohmic penalty.

Figure 8 shows the dependence of the space–time yield on the inter-electrode gap.

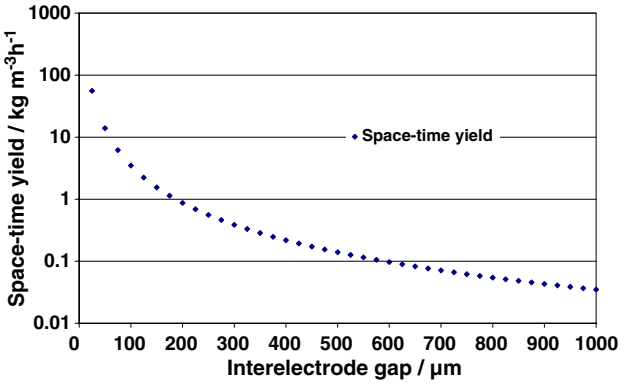

Fig. 8 A graph of the dependence of the space–time yield for $\beta = 0.90$; $M_P = 0.182$ kg mol^{-1}; $\overline{C}_A = 2$ mol L^{-1} over the inter-electrode gap

For high overpotentials a limiting current density, corresponding to the maximal possible mass transfer is obtained:

$$i_{A\,\mathrm{lim}} = zFk_mC_A. \tag{18}$$

The average space–time yield is:

$$\overline{\rho_{ST}} = \tau^{-1} \cdot \overline{C}_A\left(1 - \mathrm{e}^{-\overline{k_m}\mathrm{a_e}\tau}\right) \tag{19}$$

where the term $\overline{k_m}\mathrm{a_e}\tau$ corresponds to the Number of Transfer Units, $NTU = \overline{k}_m \cdot A_e/V_f$.

Because $\mathrm{a_e}$ of the micro reactor (which is 40,000–10,000 m^{-1}) is extremely high in comparison to conventional mono polar reactors (10 m^{-1}), to bipolar reactors (100 m^{-1}) and to a fixed bed reactor (2,000 m^{-1}). It is implicitly described by Eq. 19 that high NTU numbers are necessary in single-pass, high conversion microreactors. Due to economic factors, large scale processes are generally driven close to the transport-limited rate [44].

Equation 17 must be corrected by the electrode thickness d_e so that $\mathrm{a_e} = A_e/V_R = (d + d_e)^{-1}$.

The space–time yield Eq. 15 for instance would be:

$$\rho_{ST,corr.} = \frac{M_P i\beta}{zF(d + d_e)} \tag{20}$$

where $(d + d_e)$ is the length of the "bipolar unit". In the case of a monopolar stack reactor the total cell volume must be taken into account [23].

Therefore higher space–time yields also require thin electrodes, gaskets and low total reactor volumes. If the ratio of V_R active/V_R passive (where passive reactor volume is the reactor volume where no electrolysis has taken place) is low, the reactor becomes expensive.

In the case of an integrated heat exchanger within the electrodes then the space–time yield calculation is more complex.

2.5 Energy consumption, investment and process costs

The specific electrical energy consumption ω is defined as the ratio of the required energy per product mass

$$\omega = \frac{zFE_{cell}}{M_p\beta}. \tag{21}$$

In general there is substantial interest in keeping the investment and process costs low. Equation 22 illustrates the relationship of the optimum current density to the material and current costs [40].

$$i_{opt} = \sqrt{\frac{a_{inv} + b_{inv}W}{b_{inv}R_{cell}}} \tag{22}$$

where a_{inv} are the specific investment costs (€/cm^2 h) i.e. costs per unit surface and time; b_{inv} the current costs (€/kW h), W the efficiency of the pumps and R_{cell} the cell resistance.

2.6 Heat balance in ECMRs

The cell voltage is a complex quantity which depends not only on the electrode potentials (cathodic and anodic equilibrium- and overpotentials) but also on the ohmic potential drops IR_{drop} which are related to the current flow through the cell and the electrical circuit [36]:

$$E_{cell} = E_e^c - E_e^a - |\eta^c| - |\eta^a| - IR_{cell} - IR_{circuit}. \tag{23}$$

Equation 26 gives the thermoneutral cell voltage E_{tn}, i.e. the cell voltage which permits isothermal operation

$$E_{tn} = -\left(\frac{\Delta H}{nF}\right). \tag{24}$$

A portion E_D of the cell voltage in excess of the thermoneutral voltage equation 25

$$E_D = E_{cell} - E_{tn} \tag{25}$$

provides an electrical power loss Q:

$$Q = IE_D \tag{26}$$

which results in heating in the cell.

The ohmic drop, as defined by Eq. 2, frequently represents an important fraction of the cell voltage and plays a major role in the heat generation terms.

This is especially true in organic electrosynthesis where current densities are high and electrolyte conductivities low. A major concern of electrochemical engineering is clearly linked to the design of cells with minimum ohmic drops [44].

As a result of the construction of the ECMR, i.e. the small channels and the low inter-electrode distance in connection with the bifunctionality of the cathode (electrode with an integrated heat exchanger), the average heat

transfer coefficient a_m is analogous to the already reported high average mass transfer coefficient k_m [45, 46]. Also due to the rapid heat transfer, an ECMR constructed in such a manner also performs with a high degree of uniformity so that no hot spots occur.

3 Selected applications

3.1 Electroorganic synthesis of anisaldehyde

Initial experiments were made with a multichannel thin layer cell (ECMR-model of an inter-electrode distance of 25 µm) [10, 47]. Table 2 gives a brief overview of the ECMR-25 µm dimensions, the process parameters and results.

To investigate the features of this electrochemical microreactor, the anodic oxidation of 4-methylanisol to 4-methoxybenzaldehyde, as shown in Fig. 6, was chosen as a benchmark and was carried out under various reaction conditions. 4-Methoxybenzaldehyde (anisaldehyde) is a bulk product, produced electrochemically by BASF. The results were monitored by HPLC-analysis.

With the ECMR for low concentrations (0.1 mol L^{-1}) in methanol it was possible to increase, with short residence times, the conversion (98%), the yield (79–82%) and the selectivity (95%) using a cell voltage of 4.5–5 V and current density of 0.79 kA m^{-2} if the auxiliary electrode (cathode) was taken as reference electrode. Increasing the cell voltage increases the current, and simultaneously the conversion rises to 100%, with selectivity decreasing due to an increasing amount of side reactions as shown in Fig. 9 [10]. In the case of concentrated solution of 20 vol% (≅2 M) 4-methoxytoluene in methanol, the applied current density amounts to 19.5 kA m^{-2} (galvanostatic). The dependence of conversion and yield on the operating

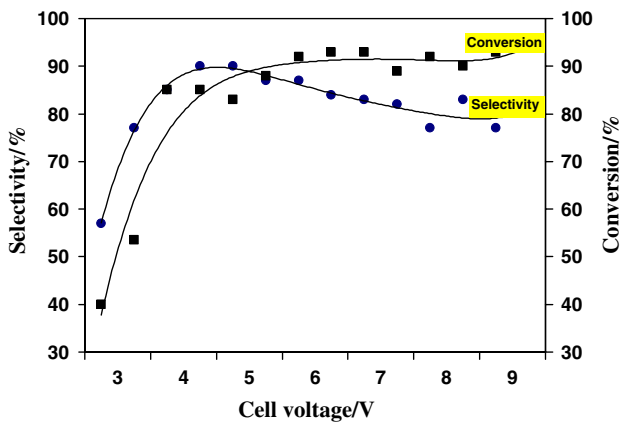

Fig. 9 Dependence of *filled square* conversion and *filled circle* selectivity on cell potential with 0.1 M KF and 0.1 M 4-methoxytoluene at ambient temperature [10]

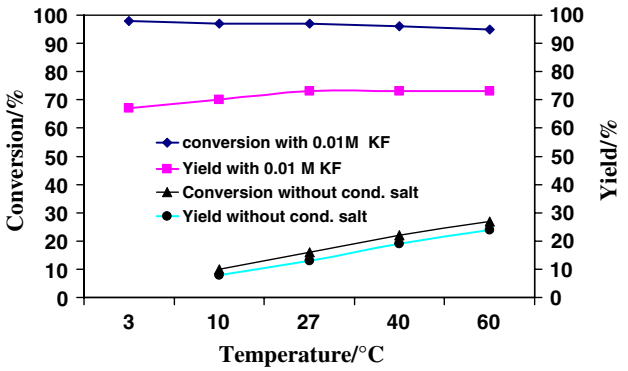

Fig. 10 Conversion and yield of 4-methoxy-benzaldehyde-dimethylacetal versus temperature and conductivity salt concentration by 4-methoxy-toluene. Reaction conditions: 20 vol% ≈2 M 4-methoxy-toluene and flow rate 1.67 × 10^{-9} m^3 s^{-1} [10]

temperature is shown in Fig. 10. When no conductivity salt is included in the electrolyte system, electrolysis occurs at higher cell voltage (>7 V).

As previously mentioned, the four-electron anodic methoxylation of 4-methoxy-toluene is currently performed by BASF with a production rate of anisaldehyde of 3,500 tons per year [27]. The electrolysis step is performed in a capillary-gap cell as shown in Fig. 2 operated in a continuous mode and placed in a recycle loop. The corresponding production scheme and the continuous process diagram including the separation steps is given in [21].

Table 3 compares typical parameters of the industrial process [21], to optimum parameters which were investigated in the framework of the EU project, IMPULSE, using the high pressure cell ECMR-100 µm (ELMI®, second version, IMM, Germany, see Sect. 2.2.2) [35]. The performance of the high pressure cell is equivalent to that of the industrial process in terms of current density, selectivity and yield. These results were obtained, even though the concentration of the supporting electrolyte had been drastically reduced by a factor of about 10. Moreover, the operating point of the high pressure cell was not optimized, as the reagent concentrations were quite low (7.5 mass% compared to 10–25 mass% for the industrial process). Furthermore, the material yield of the single-pass high conversion cell could be easily increased to 90% when recycling the 10% reagent which was not converted.

3.2 Electrolysis without supported electrolyte

3.2.1 Methoxylation of 4-methoxytoluene

The single-pass electrolysis in the absence of supporting electrolyte occurs at higher cell voltage but no additional work up to remove the conductivity salt was necessary [10].

Although the conversion (27%) and the yield (24%) for 2 M reagent concentration were low the product selectivity (≥90%) was high, as shown in Fig. 10. In this case it is not clear if the methoxy anions formed at the cathode act only as supporting electrolyte or are additionally oxidised to methoxy radicals, after diffusion or migration to the anode, to form an additional reagent.

3.2.2 *Reduction of olefins*

Marken and co-workers reported a micro flow cell with thin layer geometry with working and auxiliary electrodes directly facing each other. This arrangement allows electrosynthetic processes to be conducted in flow-through mode [11]. At sufficiently small cell height, the two diffusion layers of working and auxiliary electrode overlap or become 'coupled'. As a result electro-generated acids or bases are instantaneously neutralised, products from anode and cathode can interact and, more importantly, bulk electrolysis is possible without intentionally added electrolyte. In this preliminary report, the operation of a micro-flow cell with coupled diffusion layers is demonstrated for the one electron oxidation of ferrocene and for the two electron–two proton reduction of tetraethyl ethylenetetracarboxylate dissolved in ethanol as shown in Fig. 11. In proof-of-principle experiments omitting added electrolyte, high yields of the product, tetraethyl ethanetetracarboxylate were obtained at a nickel working electrode as summarised in Table 4. It was demonstrated that a sufficient concentration of electrolyte for bulk electrolysis is generated locally and in situ between working and auxiliary electrode.

The same author reported the electrolyte free cathodic dimerisation of 4-nitrobenzylbromide in a micro-gap flow cell [14]. The electrochemical reduction of 4-nitrobenzylbromide was studied in *N*,*N*-dimethylformamide solution in the presence and absence of intentionally added supporting electrolyte. By conventional voltammetry, it was shown that an ECE-type reaction (E = electrochemical step, C = chemical step) occurs with formation of the dimer 4,4′-dinitrodibenzyl, irrespective of the presence of supporting electrolyte. Subsequently, a micro-gap flow cell was employed for the preparative electro-reduction in the absence of supporting electrolyte. Excellent yields of the dimer were obtained and explained based on a self-propagation mechanism.

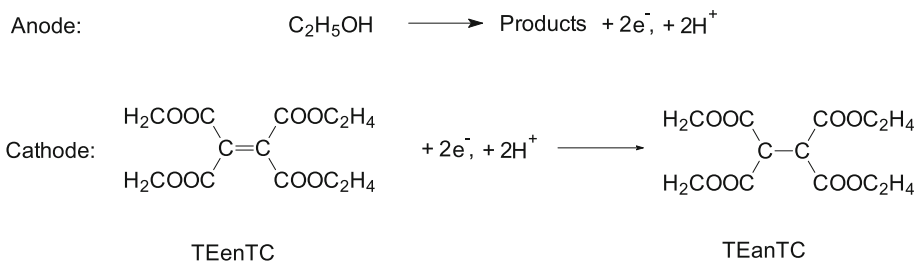

Fig. 11 Cathodic reduction of tetraethyl ethylenetetracarboxylate in ethanol [11]

Table 4 Data from electrolysis experiments with micro-flow cell systems for the reduction of tetraethyl ethylenetetracarboxylate [14]

Entry	Electrolyte $LiClO_4$ (10^3 mol m^{-3})	TEenTC (10^3 mol m^{-3})	V_f (10^{-12} m^3 s^{-1})	Current (10^{-3} A)	Yield (%)
Micro-flow cell with Ni working/Pt auxiliary electrode (width 0.5 × 10^{-2} m, length 0.5 × 10^{-2} m, height 1 × 10^{-4} m)					
1	0.1	0.02	31.7	−1.0	60
2	0.1	0.02	317	−1.5	30
Micro-flow cell with Ni working/Pt auxiliary electrode (width 0.5 × 10^{-2} m, length 2.5 × 10^{-2} m, height 1 × 10^{-4} m)					
3	0.1	0.02	31.7	−2.0	86
4	0.1	0.02	158	−3.5	20
5	0.1	0.02	317	−4.3	10
6	0.0	0.02	31.7	−1.0	60
7	0.0	0.02	158	−2.8	30
8	0.0	0.02	317	−3.5	10
9	0.0	0.01	31.7	−1.2	92
10	0.0	0.01	158	−1.5	7
11	0.0	0.01	317	−2.0	4

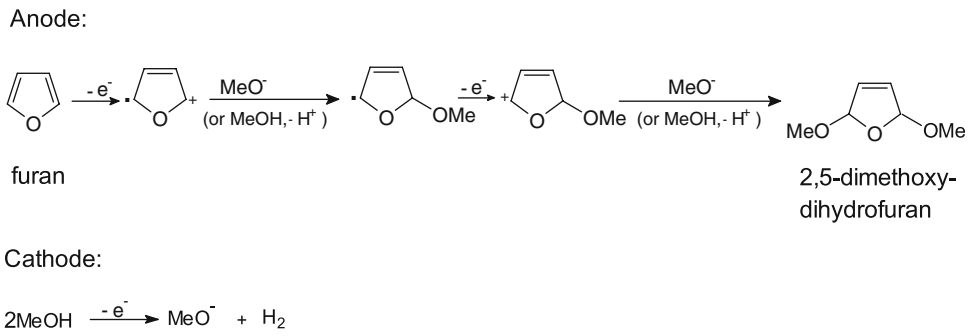

Fig. 12 Paired electrolysis of furan to 2,5-dimethoxy-2,5-dihydrofuran without supporting electrolyte [13]

3.2.3 *Direct electrolysis of furan to 2,5-dimethoxy-2,5-dihydrofuran*

Atobe and co-workers [16] reported the self-supported paired electrosynthesis of 2,5-dimethoxy-2,5-dihydrofuran using a thin layer flow cell without added supporting electrolyte. The 2,5-dimethoxy-2,5-dihydrofuran, as shown in Fig. 12, was prepared by the oxidation of furan and by the reduction of methanol solvent using a thin layer flow cell with anode and cathode directly facing each other and without intentionally added electrolyte. Controlling factors for this kind of self-supported paired electrosynthesis, such as the electrode material, the current density and the flow rate were optimized. The maximum chemical yield of 98% of pure product without work-up could be obtained with a combination of a glassy carbon anode and a platinum cathode in a single pass of furan solution.

The thin layer flow cell was constructed from platinum plates (3×10^{-2} m width, 3×10^{-2} m length) and/or glassy carbon plates (3×10^{-2} m width, 3×10^{-2} m length). A spacer (both sides adhesive tape, 80 μm thickness, Nitto Denko, Japan) was used to leave a rectangular channel exposed, and the two electrodes were simply sandwiched together ($A_e = 1 \times 10^{-2}$ m width, 3×10^{-2} m length) as shown in Fig. 3. After connecting Teflon tubing to the inlet and outlet, the cell was sealed with Epoxy resin. In Table 5 the performance of chemical and electrochemical processes are compared.

Table 5 Comparison of the performance between the chemical and electrochemical operations for the production of 2,5-dimethoxy-2,5-dihydrofurane [15, 16, 34]

	Conventional [34]	Electrochemical (conventional) [15]	ECMR directly (i.e. without conductivity salt) [16]
Yield (%)	70–75	80–85	98%
Current efficiency (%)	–	85	10%
Current density (kA m^{-2})	–	1.5	0.1
Energy consumption (kWh kg^{-1})	–	3	Unknown

3.2.4 *Paired electrolysis of toluene and acetophenone using a micro-flow reactor*

Atobe and co-workers also developed a paired electrosynthetic system using a microflow reactor without intentionally added electrolyte [48]. This system enables paired electrochemical reactions of chloride reduction/alcohol oxidation progressing without added electrolyte. In addition, the use of parallel laminar flow in the microflow reactor resulted in further improvement of the desired product yields (35% toluene and 70% acetophenone) in the paired electrosynthesis as shown in Fig. 13. The experiments were conducted in a microreactor composed of a silver cathode and indium-tin oxide (ITO) anode (Fig. 3).

3.2.5 *Paired electrochemical synthesis of 2,3-butanediol to 2-butanone in undivided flow cells*

Baizer et al. developed a procedure for converting 2,3-butanediol (A) in ca. 10% aqueous solution to 2-butanone (C) by passing it through a porous anode at which it was selectively oxidized to acetoin (B) by electrogenerated

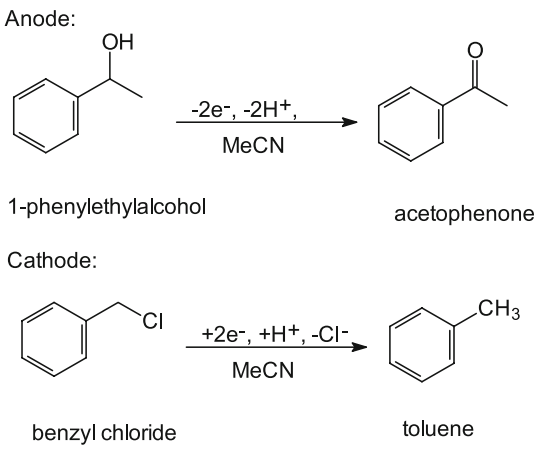

Fig. 13 Paired electrolysis of toluene and acetophenone using a micro-flow reactor [48]

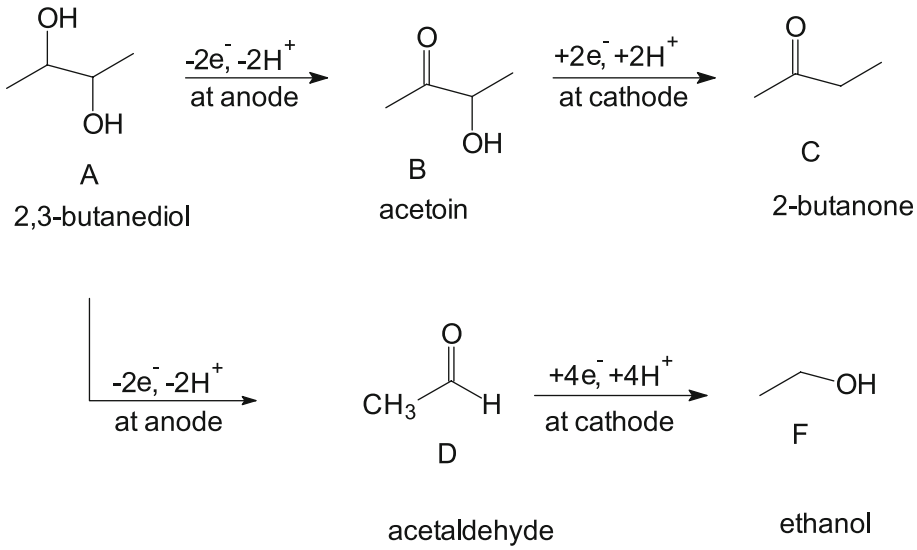

Fig. 14 Paired electrochemical synthesis of 2-butanone in undivided flow cell [49]

NaBrO and then pumped to a porous cathode at which it was reduced to 2-butanone [3]. The not fully optimized yields and current efficiencies were 75% and 60%, respectively. The procedure employed Pb/Hg or Zn/Hg cathodes, graphite anodes, pH of about 7, ambient temperature, current density of 20 A m^{-2}, five minute residence time outside the cell, packed bed electrodes, and parallel electrolyte and current flow.

For the same synthesis as shown in Fig. 14, Atobe and co-workers constructed a microcell comprising of a Pt or PbO_2 anode and Pb cathode of 1 cm × 3 cm area and interelectrode distance of 80 μm as shown in Fig. 3. For 150 A m^{-2} (constant current density in different conditions described in Table 6) moderate yields were obtained by operation without supporting electrolyte [49]. When supporting electrolytes were used poor results were achieved.

3.2.6 *Anodic substitution reaction of cyclic amine with allyltrimethylsilane*

Atobe and co-workers again developed a novel electrosynthetic system for anodic substitution reactions by using parallel laminar flow in a microflow reactor. This system enables nucleophilic reactions to overcome the restraint, such as the oxidation potential of nucleophiles and the stability of cationic intermediates, by the combined use of ionic liquids as reaction media and the parallel laminar flow in the microflow reactor [50]. By using this novel

Table 6 Paired electrosynthesis of 2-butanone and ethanol from 2,3-butanediol [49]

Supporting electrolyte	Flow rate (10^{-10} m^3 s^{-1})	Anode material	Cathode material	Yield			Conversion (%)
				B (%)	C (%)	F (%)	
0.5 M Na_2SO_4	1.67–8.3	PbO_2	Pb	Trace amount-2	1–5	1–4	80–94
0.5 M Na_2SO_4	1.67–8.3	Pt	Pb	Trace amount-2	3–5	1–4	64–96
None	1.67–8.3	Pt	Pb	Trace	0–1	21–30	67–84

Concentration of A: 3 mM

Current density 150 A m^{-2}

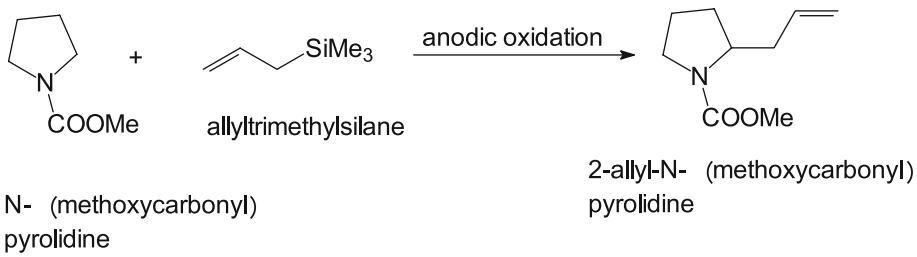

Fig. 15 Anodic substitution reaction of *N*-(methoxycarbonyl)pyrolidine with allyltrimethylsilane [50]

Table 7 A summary of the anodic substitution reaction experiments of *N*-(methoxycarbonyl)pyrolidine with allyltrimethylsilane in the parallel laminar mode [50]

Experiment	Electrolytic solution	Conversion of 1 (%)	Yield of 3 (%)
1	0.1 M n-Bu_4NBF_4/MeCN	73	0.6
2	0.1 M n-Bu_4NBF_4/TFE[a]	58	59
3	[emin][BF_4][b]	61	62
4	[emin][TFSI][c]	66	73
5	[deme][TFSI][d]	54	91

The flow rates of the two electrolytic solutions containing A and B, respectively, were fixed at 0.1 mL min^{-1} each. Current density was 30 A m^{-2} and the reaction temperature was at 20 °C

[a] TFE 2,2,2-trifluoroethanol

[b] [emin][BF_4] for 1-ethyl-3-methylimidazonium tetrafluoroborate

[c] [emin][TFSI] for 1-ethyl-3-methylimidazonium bis(trifluoromethanesulfonyl)imide

[d] [deme][TFSI] for *N*,*N*-diethyl-*N*-(2-methoxyethyl)ammonium bis(trifluoromethanesulfonyl)imide

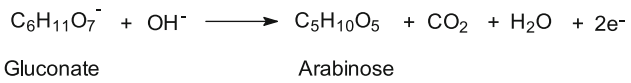

Fig. 16 Anodic formation of arabinose in alkaline medium [51]

electrosynthetic system, the anodic substitution reaction of carbamates, especially of cyclic carbamates, with allyltrimethylsilane, as shown in Fig. 15, were carried out to provide the corresponding products in moderate to good yields as shown in Table 7 in a single flow-through operation at ambient temperature (without the need for low-temperature conditions).

3.2.7 Anodic decarboxylation of glyconate to arabinose

Schmidt-Traub and co-workers reported a new continuous process, combining electrochemical reaction and chromatographic simulated-moving-bed (SMB) separation [51]. For the development of this novel continuous process the electrochemical reaction, took place in an ECMR which was then coupled to the SMB plant. To demonstrate the potential of process integration, this reactor concept was applied to the direct electrochemical production of arabinose as shown in Fig. 16 by means of simulation. Experimentally verified models of 'reactor' and 'column' units are combined with a model of the electrochemical SMB-reactor. These process units are characterized individually and their model parameters are discussed. The electrochemical reaction inside the microreactor can be described by a series of reactions, which has an impact on the design of the integrated process. As the reaction should take place in areas of the SMB-process with maximum educt concentration, the reactors are switched 'on' and 'off' during operation. The integrated process shows interaction between reaction and separation so as to diminish side reactions. Case studies prove the theoretical feasibility of the integrated process. Compared to a process with conventional reactors utilisation of an integrated ECMR/SMB-separation system leads to the attainment of higher yields (48% for 99% product purity).

4 Conclusions

Generally many advantages of the flow reactors which work under hydrodynamic control conditions can be improved by the application of microreactors. These are:

- The continuously flowing electrolyte removes the reaction products and impurities from the electrode surface and conditions the electrodes.
- During the electrolyte flow a continuous replenishment of the Nernst diffusion layer δ_N takes place over the electrode.

Electro-chemical micro reactors provide additional operational advantages compared with conventional reactors such as:

- The high specific area of the ECMR allows operation in a single-pass high conversion mode, leading to a continuous process without recycle. This process scheme has two major advantages over classical process flow schemes: it requires only a small separation unit and both the short residence time and plug flow of the reagent, minimize undesired side reactions which lead to higher current yields and better product qualities.
- In the case of gas evolution at electrodes of conventional reactors the coalescence and growth of gas bubbles is inevitable. This leads to the formation of a heterogeneous electrolyte system with low conductivity and a higher resistance and a higher cell voltage, with corresponding electrical energy losses as Joule heat. This temporary or permanent occupancy of either part of the electrode surface or the electrolyte volume by gas bubbles leads to a reduced performance. The coalescence and growth of gas bubbles is inhibited for microreactors with interelectrode distance as low as 50 μm.
- The space–time yield is generally an order of magnitude higher than that of conventional cells if, in addition to the reduced electrode gap, the electrodes themselves are thin.
- Operation with electrolytes of low conductivity and/or in the absence of conductivity salt is possible.
- In the case of conventional electrolysis reactors, it is often difficult to predict the heat transfer quantitatively

due to the variety of materials used in cell construction and the (sometimes) complex geometry. In such cases, ECMR as a laboratory tool may provide useful opportunities to measure heat transfer and hence establish an operational heat balance.

- In flow-through cells the electrolyte acts as a heat-exchanger fluid. The additional integrated heat exchanger directly on the electrodes allows not only fast heat transfer but also operation at quasi isothermal conditions. Therefore, no hot spots should occur, thus leading to optimum control of reaction conditions.
- ECMRs allow operations with higher current densities in combination with lower specific energy consumption.
- Material costs are much lower with higher safety and more convenience in operation.
- The serial application of continuous microextractors with separation units such as Simulated Moved Bed (SMB) chromatography or micro distillation plant is possible.

Microreactors also have some disadvantages:

- The coupling of the diffusion zones may lead to the following problems: Mixing of oxidation and reduction products occurs with possibly uncontrolled follow-up chemistry. In the undivided cells the product formed at the working electrode may be converted back/further by reaction at the counter electrode.
- Because only a few electrochemical syntheses have been realised to-date in thin-gap high-conversion flow cells, there are currently neither investments nor process cost calculation reports in the literature. As previously mentioned, only a few examples are known with concentrations similar to the conditions in industrial processes. Most of the investigations have been performed in conditions which are not relevant for commercial production purposes: diluted media and low average current densities.

In summary, it is clear that ECMRs represent an advance on conventional reactors and show promise for future application in the field of organic synthesis. Therefore much work must be performed to ensure that technical and economic improvements are achieved and transferred to organic synthesis applications.

References

1. Stulik K (1987) Pure Appl Chem 59:521
2. Kellner R, Mermet JM, Otto M, Valcarcel M, Widmer HM (2004) Analytical chemistry: a modern approach to analytical science, 2nd edn. Wiley-VCH Verlag & Co. KGaA, Weinheim
3. Baizer MM, Nonaka T, Park K, Saito Y, Nobe K (1984) J Appl Electrochem 14:197
4. Degner D (1988) Organic electrosynthesis in industry. In: Topics in current chemistry. Springer-Verlag, Berlin, p 148
5. Lund H, Hammerrich O (2001) Organic electrochemistry, 4th edn. Marcel Dekker, New York
6. Schultze JW, Tsakova V (1999) Electrochim Acta 44:3605
7. Hessel V, Hardt S, Löwe H (2004) Chemical micro process engineering. Wiley-VCH, Weinheim
8. Löwe H, Küpper M, Ziogas A. Reactor and method for carrying out electrochemical reactions, WO/2000/015872
9. Ziogas A. Process for carrying out electrochemical reactions using a microreactor, EP1217099
10. Ziogas A, Löwe H, Küpper M, Ehrfeld W (2000) Electrochemical microreactors: a new approach for microreaction technology. In: Ehrfeld W (ed) Microreaction technology: industrial prospects, IMRET 3: proceedings of the 3rd international conference on microreaction technology, Frankfurt/Main. Springer Verlag, Berlin, p 136
11. Paddon CA, Pritchard GJ, Thiemann T, Marken F (2002) Electrochem Commun 4:825
12. He P, Watts P, Marken F, Haswell SJ (2005) Electrochem Commun 7:918
13. Horii D, Atobe M, Fuchigami T, Marken F (2005) Electrochem Commun 7:35
14. Horii D, Atobe M, Fuchigami T, Marken F (2006) J Electrochem Soc 153:143
15. Belmont C, Girault HH (1995) Electrochim Acta 40:2505
16. Paddon CA, Atobe M, Fuchigali T, He P, Watts P, Haswell SJ, Prichard GJ, Bull SD, Marken F (2006) J Appl Electrochem 36:617
17. Bond AM, Fleischmann M, Robinson J (1984) J Electroanal Chem 168:299
18. Märkle W, Speiser B, Tittel C, Vollmer M (2005) Electrochim Acta 50:2753
19. Erichsen T, Reiter S, Märkle W, Tittel C, Ryabova V, Bonsen EM, Jung G, Speiser B, Schuhmann W (2005) Rev Sci Instrum 76:062204
20. Pütter H (2001) Industrial electroorganic chemistry, 4th edn. Marcel Dekker, New York
21. Hamann CH, Hamnett A, Vielstich W (1998) Electrochemistry. Wiley-VCH, Weinheim
22. Wendt H, Kreysa G (1999) Electrochemical engineering, science and technology in chemical and other industries. Springer-Verlag, Berlin
23. Beck F (1987) Organic electrosynthesis, Ullmann's encyclopedia of industrial chemistry. VCH verlagsgesellschaft mbH, Weinheim
24. Pletcher D, Walsh FC (1990) Industrial electrochemistry, 2nd edn. Chapman-Hall, London
25. Jüttner K (2004) Encyclopedia of electrochemistry, 1st edn. Wiley-VCH, Weinheim
26. Beck F, Guthke H (1969) Chem Ing Tech 41:943
27. Ohno H (2005) Electrochemical aspects of ionic liquids. Wiley, New York. ISBN:978-0-471-64851-2
28. Wendt H, Bitterlich S, Lodowicks E, Liu Z (1992) Electrochim Acta 37:1959
29. Sekiguchi K, Atobe M, Fuchigami T (2002) Electrochem Commun 4:881
30. Degner D, Barl M, Siegel H, DE2848397
31. Jörissen J (2004) Practical aspects of preparative scale electrochemistry, encyclopedia of electrochemistry. In: Schäfer H (ed) Organic electrochemistry. Viley-VCH, Weinheim
32. Wendt H, Bittterlich S (1992) Electrochim Acta 37:1951
33. Attour A, Rode S, Ziogas A, Matlosz M, Lapicque F (2008) J Appl Electrochem 38:339

34. Bersier BM, Carlsson L, Bersier J (1994) Topics in current chemistry. Springer-Verlag, Berlin
35. EU FP6 Project Impulse (2005) contact no. NMP2-CT-2005-011816
36. Kapałka A, Lanova B, Baltruschat H, Fóti G, Comninellis C (2008) Electrochem Commun 10:1215
37. Kapałka A, Fóti G, Comninellis C (2008) Electrochem Commun 10:607
38. Bellagamba R, Michaud PA, Comninellis C, Vatistas N (2002) Electrochem Commun 4:171
39. Attour A, Rode S, Bystron T, Matlosz M, Lapicque F (2007) J Appl Electrochem 37:861
40. Schmidt VM (2003) Elektrochemische Verfahrenstechnik. Wiley-VCH Verlag GmbH & KGaA, Weinheim. ISBN:3-527-29958-0
41. Rode S, Altmeyer S, Matlosz M (2004) J Appl Electrochem 34:678
42. Rode S, Attour A, Lapicque F, Matlosz M (2008) J Electrochem Soc 155:193
43. Attour A, Rode S, Lapicque F, Ziogas A, Matlosz M (2008) J Electrochem Soc 155:201
44. Pickett DJ (1979) Electrochemical reactor design, 2nd edn. Elsevier, New York
45. Beek WJ, Muttzall KMK, van Heuven JW (1999) Transport phenomena, 2nd edn. Wiley, England
46. Polyanin AD, Kutepov AM, Vyazmin AV, Kazenin DA (2002) Hydrodynamics, mass and heat transfer in chemical engineering. Taylor & Francis, London. ISBN:0-415-27237-8
47. Küpper M, Löwe H, Ziogas A (1998) GDCh-Monographie 14:435
48. Amemiya F, Horii D, Fuchigami T, Atobe M (2008) J Electrochem Soc 155:E162
49. Horii D, Atobe M, Fuchigami T, Marken F (2004) Abstracts of the 206th meeting of the Electrochemical Society, p 2144
50. Horii D, Amemiya F, Fuchigami T, Atobe M (2008) Chem Eur J 14:10382
51. Michel M, Schmidt-Traub H, Ditz R, Schulte M, Kinkel J, Stark W, Küpper M, Vorbrodt M (2003) J Appl Electrochem 33:939
52. Vračar LM, Gojković SL, Elezović NR, Radmilović VR, Jakšić MM, Krstajić NV (2006) J New Mater Electrochem Syst 9:99
53. Smith JR, Walsh FC, Clarke RL (1998) J Appl Electrochem 28:1021
54. Farndon EE, Pletcher D (1997) Electrochim Acta 42:1281